

Simulation and meta-modeling of electron beam welding using genetic algorithms

K. Mohanty, G. G. Roy, N. Chakraborti

Multi-objective evolutionary and genetic algorithms based meta-models were constructed for the electron beam welding process of 304L stainless steel. The meta-models were data-driven and based upon the results of extensive transport phenomena based numerical simulations of the process. The accuracy of the meta-model predictions was confirmed experimentally.

KEYWORDS: ELECTRON BEAM WELDING - STAINLESS STEEL - MODELING - OPTIMIZATION - SIMULATION - GENETIC ALGORITHMS - TRANSPORT PHENOMENA

INTRODUCTION

In recent years Electron Beam Welding (EBW) has found its multi-faceted applications in various fields like automobiles, aerospace and nuclear industries [1]. This paper presents an attempt to simulate the electron beam welding of 304L stainless steel, commonly referred as '18/8 stainless steel' and contains around 18% chromium and 8% nickel, along with a maximum of 0.030% carbon.

The physical and microstructural characteristics of such steels are readily available in the standard literature [2].

The modeling and optimization strategy includes an elaborate transport phenomena based approach and then to construct more manageable but acceptably accurate meta-models out of the simulated data. The predicated trends are verified through limited experimentation. The details are provided below.

MODELING THE KEYHOLE

Highly energetic electron beams give off their kinetic energy after heating a metallic surface through a series of collisions with the metal atoms or molecules. The thermal energy released through the process raises the temperature to a level high enough to cause melting and evaporation. The electron beam then penetrates inside the molten metal and a nail shaped hole called keyhole is formed.

The keyhole gets filled with the ionized metal atoms or plasma and that results in scattering of the electron beam. The liquid metal pool from the surrounding almost immediately fills up the keyhole as the beam traverses away from it and sound weld joint results upon solidification. A typical keyhole observed experimentally during this study for 304L stainless steel is shown in Figure 1.

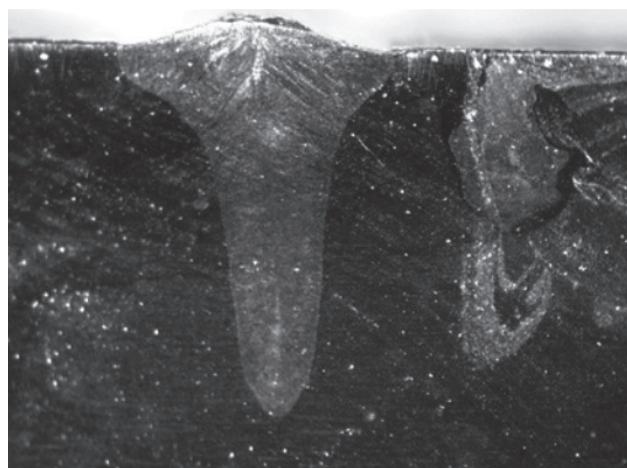


Fig. 1 - Experimentally observed keyhole formation in 304L stainless steel. Input power: 3250 W. Welding speed: 1.83 cm.s⁻¹. Aspect ratio of pool: 1.36

The model used here was developed earlier [3] and it calculates the three dimensional temperature and velocity fields in a liquid metal weld pool in a steady state keyhole mode welding. In this study the keyhole surface is assumed to be at the boiling point of the steel being welded.

The crucial task of calculating the keyhole profile is accomplished iteratively through a point by point energy balance on the pool surface.

**Kaibalya Mohanty, Gour Gopal Roy,
Nirupam Chakraborti**

*Department of Metallurgical & Materials Engineering
Indian Institute of Technology,
Kharagpur 721 302, India*

The computed keyhole profile is the mapped onto a three dimensional calculation domain for the subsequent computation of fluid flow and heat transfer in the liquid and the solid-liquid regions. The model generated a data set of the welding process consisting of the pool geometry parameters i.e. length, depth and half width of the metal pool created during the welding as a function of the variables and their ranges shown in Table 1. The electron beam defocus is another parameter which could be adjusted in the model. Here, for convenience, it was set to zero for all simulations, implying that the electron beam is focused exactly at the surface of the work piece; not above (negative defocus) or below (positive defocus), as those might result in a non-uniform trend in the weld pool geometry. The mathematical details of the model are as follows:

Phenomenological model of keyhole mode welding:

In this investigation the shape of the keyhole, as stated before, is generated by conducting a point by point heat balance on the keyhole surface, which is then mapped onto a thermo-fluid code

$$S_j = -\frac{\partial p}{\partial x_j} + \frac{\partial}{\partial x_i} \left(\mu \frac{\partial u_j}{\partial x_j} \right) - C \left(\frac{(1-f_L)^2}{f_L^3 + B} \right) u_j + \rho g \beta (T - T_r) \quad (2)$$

where p denotes the pressure, f_L denotes the liquid fraction, B is a very small positive constant that safeguards against any division by zero, C is a constant taking into account the mushy zone morphology, β denotes the coefficient of volume expansion of the liquid, and T_r is taken as a reference temperature, while U denotes the welding velocity.

The terms in the right hand side represent the pressure drop, frictional dissipation in the mushy zone that forms during the process, a buoyancy term along with a structural component of momentum that could not be directly assimilated in eq.(1).

The continuity equation:

$$\frac{\partial(u_i)}{\partial x_i} = 0 \quad (3)$$

A one equation viscosity model is coupled with momentum equations in this study, which ensured simplicity and fast computation.

Considering the phase change, the total enthalpy H is taken as the sum of sensible heat h and latent heat content ΔH , i.e., $H = h + \Delta H$. The sensible heat h is calculated as $h = \int C_p dT$, where C_p denotes the specific heat, and T denotes the temperature. The latent heat content ΔH is taken as $\Delta H = f_L L$, where L denotes the latent heat of fusion. The liquid fraction f_L is assumed to linearly vary with temperature between the liquidus, T_L , and solidus, T_S , temperatures such that:

to simulate the flow configuration surrounding the wall of the keyhole, taking it as a rigid body [3]. Here the calculations are made using a coordinate moving along with the heat source. The calculations are made assuming steady state after the heat source moves a small distance from the edge of the material, assuming an incompressible and laminar Newtonian flow in the weld pool. The relevant 3-D momentum equations are presented in eq.(1).

$$\rho \frac{\partial u_j}{\partial t} + \rho \frac{\partial(u_i u_j)}{\partial x_i} = \frac{\partial}{\partial x_i} \left(\mu \frac{\partial u_j}{\partial x_i} \right) + S_j \quad (1)$$

where, u denotes the velocity, i and j represent x, y, z Cartesian orthogonal directions indexed as 1, 2, and 3, respectively, ρ denotes the density, t and μ are time and the viscosity respectively. S_j is a momentum source term in the j direction, expressed as:

$$f_L = \begin{cases} 1 & T > T_L \\ \frac{T - T_S}{T_L - T_S} & T_S \leq T \leq T_L \\ 0 & T < T_S \end{cases} \quad (4)$$

The thermal energy transport in the weld workpiece is expressed by a modified energy equation given as:

$$\rho \frac{\partial h}{\partial t} + \rho \frac{\partial(u_i h)}{\partial x_i} = \frac{\partial}{\partial x_i} \left(\frac{k}{C_p} \frac{\partial h}{\partial x_i} \right) + S_h \quad (5)$$

where k denotes the local thermal conductivity. The source term S_h is due to the latent heat content and is expressed as:

$$S_h = - \left[\rho \frac{\partial(\Delta H)}{\partial t} + \rho \frac{\partial(u_i \Delta H)}{\partial x_i} \right] \quad (6)$$

The boundary conditions used are summarized below.

At the top surface the Marangoni stress condition is assumed. No slip condition is applied at all other solid walls including the keyhole surface. The keyhole surface is assumed to be at boiling temperature and all other boundary walls taken at the room temperature. The control volume method based SIMPLE algorithm is used for the numerical solution. Non-uniform grids are used for spatial resolution of velocity and temperature at the point of steep gradients. Further details are available elsewhere [3].

Tab. 1 - Details of the input parameters considered in the EBW model.

Process parameters	Minimum	Maximum	Step size	Number of steps
Power(Watts)	2500	5500	375	9
Beam radius(cm)	0.035	0.04	0.00125	5
Power distribution factor	2	4	1	3
Welding speed(cm/s)	0.33	3.33	0.75	5

META-MODELING

These simulations are quite elaborate and computing expensive. For quick and accurate estimation of the required properties one needs to construct simple meta-models, which by definition are the models made out of models. The original simulations require highly time consuming calculations involving eq. 1-6. If meta-models are not used, in order to optimize in an evolutionary fashion, one would require performing such very lengthy calculations several thousand times, which is computationally prohibitive. The meta-models in this case substitute the equations by a simple function, either a neural net or a tree, which can be computed very fast maintaining an acceptable level of accuracy. Two evolutionary and genetic algorithm [4] based strategies, Evolutionary Neural Network (EvoNN) [5-6] and Bi-objective Genetic Programming (BioGP) [7-8], successfully used earlier on a number of problems [9-11] were employed for this purpose to construct meta-models for the Input power and the aspect ratio of the keyhole. Both EvoNN and BioGP performed quite acceptably, as evident in Figure 2, where the model predictions are pitted against the data from the simulation experiments. Here nearly seven hundred points from the original simulation are arranged in an array, and their positions in the array are denoted as 'Data index' in the abscissa. The corresponding values obtained from the meta-model are also plotted in the same figures to provide a comparison, and in most cases agreement seems to be very good.

THE VARIABLE RESPONSES

The aspect ratio of the keyhole is one crucial parameter that directly influences the efficacy of welding. It is important to learn how it is related to the speed of welding at various power levels. To determine this, we have adopted a methodology discussed

earlier [12]. In essence, it involved keeping every variable, other than the speed of welding, in the meta-model of aspect ratio constant at a base level, and then giving the speed of welding a systematic perturbation to record the corresponding changes in the aspect ratio. Both EvoNN and the BioGP meta-models have shown the same response as shown in Figure 3. It seems that aspect ratio varies inversely with the speed of welding. In other words, an increase in the speed of welding would result in a lower value of aspect ratio and vice versa. Although, intuitively, this seems correct, an experimental confirmation was still warranted and that was attempted next.

EXPERIMENTAL VERIFICATION

During this study EBW experiments were performed with the 304L stainless steel samples. These were conducted at three different power values which were within the range of the input power initially determined (Table 1). The welding operations were done at three different welding speeds, which were again within the range initially determined. Thus, a total of nine experiments were performed.

Results (Figure 4) show that at a fixed input power value, aspect ratio of the pool created during the welding shows an increasing trend as the speed of welding decreases. In principle, this should continue till an optimum value is reached. At the welding speeds of 1.83 cm. s⁻¹ and 3.33 cm. s⁻¹ the aspect ratio increased almost linearly with the increasing power, thus quite acceptably corroborating the model predictions. At the much lower speed of 0.33 cm. s⁻¹ the 304 L stainless steel samples were actually cut, instead of being joined when the power value was raised above 4000.W. Therefore, only the result obtained at the power value of 3250W is shown in Figure 4.

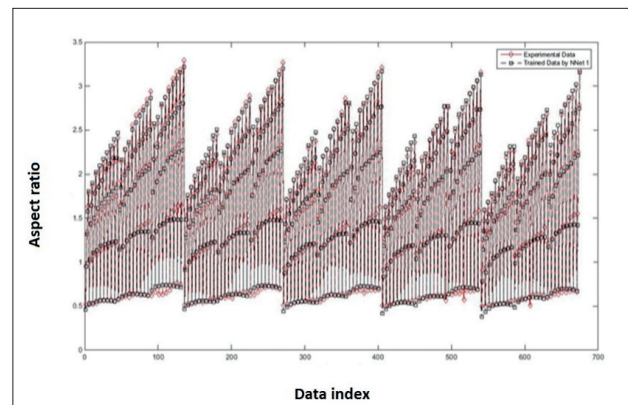
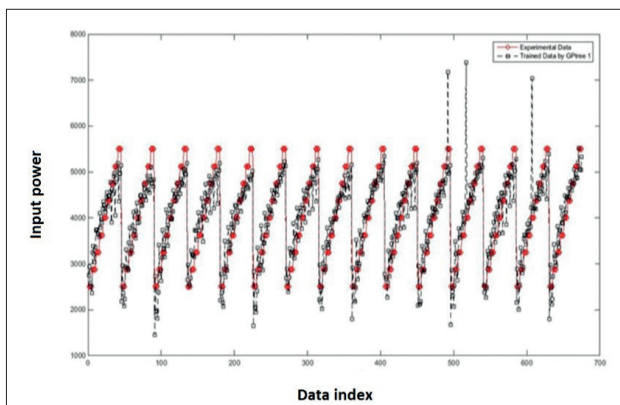


Fig. 2 - A typical fit by BioGP (left) and EvoNN (right)

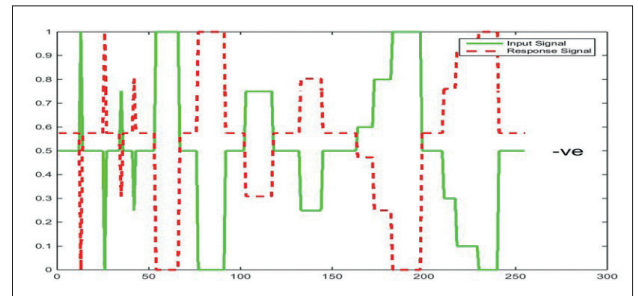
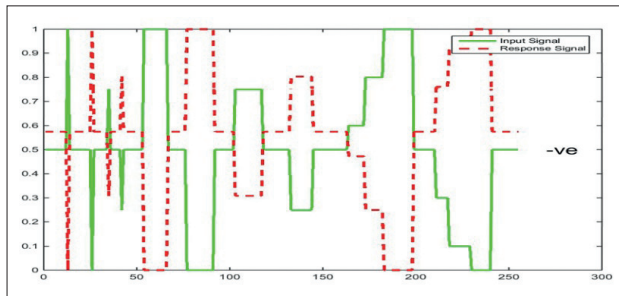


Fig. 3 - Variation of the response signal of the aspect ratio (dashed lines) with the perturbation in the input signal of the speed of welding (solid lines). Left EvoNN, right BioGP. Both the signals are normalized between 0 to 1 and the abscissa uses an arbitrary scale.

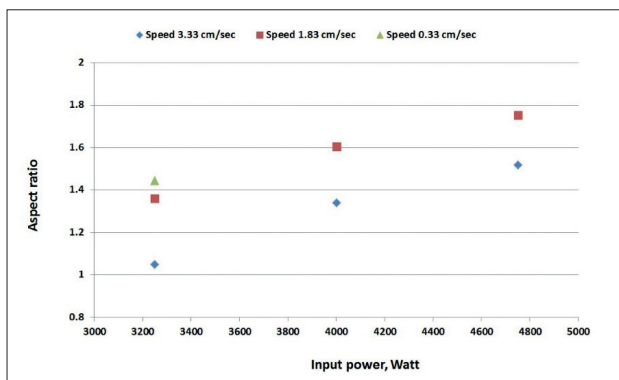


Fig. 4 - Experimental verification of the meta-model predictions.

CONCLUDING REMARKS

Data-driven evolutionary meta-models are now being increasingly used for the metallurgical processes [13-14]. In this study the successful implementation of an evolutionary algorithm-based phenomenological model for the electron beam welding process, and the experimental confirmation of the predictions therefrom can be used very effectively in any future research in this area. Contrary to the analytical models, which are often not suitable for a real life application due to many simplistic assumptions, or the rigorous numerical models that are often computationally prohibitive, the meta-models developed in this study ensure fast computation and reliable prediction and thus become very useful in a practical situation.

REFERENCES

- [1] Cottrell, C.L.M. Electron beam welding - a critical review. *Materials and design* 1985, 6(6), 285-291.
- [2] <http://www.outokumpu.com/SiteCollectionDocuments/Outokumpu-stainless-steel-handbook.pdf>
- [3] Rai, R.; Roy, G. G.; DebRoy T.; 'A computationally efficient model of convective heat transfer and solidification characteristics during keyhole mode laser welding' *Journal of applied Physics*, Volume 101, Pages 054909-1-11 (2007)
- [4] Datta, S.; Chattopadhyay, P.P. 'Soft computing techniques in advancement of structural metals', *International materials reviews*, Volume: 58 Pages: 475-504 (2013)
- [5] Pettersson, F.; Chakraborti, N.; Saxén, H. 'A genetic algorithms based multi-objective neural net applied to noisy blast furnace data', *Applied soft computing*, Volume: 7 Pages: 387-397 (2007)
- [6] Mondal, D.N.; Sarangi, K.; Pettersson, F.; Sen, P.K.; Saxén, H.; Chakraborti, N.; 'Cu-Zn separation by supported liquid membrane analyzed through Multi-objective Genetic Algorithms', *Hydrometallurgy*, Volume: 107 Pages: 112-123 (2011)
- [7] Giri, B. K.; Hakanen, J.; Miettinen, K.; Chakraborti, N.; 'Genetic programming through bi-objective genetic algorithms with a study of a simulated moving bed process involving multiple objectives', *Applied soft computing*, Volume: 13 Pages: 2613-2623 (2013)
- [8] Giri, B. K.; Pettersson, F.; Saxén, H.; 'Genetic Programming Evolved through Bi-Objective Genetic Algorithms Applied to a Blast Furnace', *Materials and manufacturing processes*, Volume: 28 Pages: 776-782, (2013)
- [9] Hariharan, K.; Chakraborti, N.; Barlat, F.; Lee, M.G.; 'A Novel Multi-objective Genetic Algorithms-Based Calculation of Hill's Coefficients' *Metallurgical and materials transactions A-Physical metallurgy and materials science* Volume: 45A, Pages: 2704-2707 (2014)
- [10] Hariharan, K.; Ngoc-Trung N.; Chakraborti, N.; Lee, M.G.; Barlat, F.; 'Multi-Objective Genetic Algorithm to Optimize Variable Drawbead Geometry for Tailor Welded Blanks Made of Dissimilar Steels', *Steel research international* Volume: 85, Pages: 1597-1607 (2014)
- [11] Halder, C.; Madej, L.; Pietrzyk, M.; Chakraborti, N.; 'Optimization of Cellular Automata Model for the Heating of Dual-Phase Steel by Genetic Algorithm and Genetic Programming' *Materials and manufacturing processes* Volume: 30, Pages: 552-562 (2015)
- [12] Chakraborti, N. 'Evolutionary data-driven modeling' in *Informatics for Materials Science and Engineering*, Rajan, K. (ed.); Butterworth-Heinemann, Oxford (2013)
- [13] Kovacic, M.; 'Modeling of Total Decarburization of Spring Steel with Genetic Programming'; *Materials and manufacturing processes* Volume: 30 Pages: 434-443 (2015)
- [14] Lestan, Z.; Klancnik, S.; Balic, J.; Brezocnik, M.; 'Modeling and Design of Experiments of Laser Cladding Process by Genetic Programming and Nondominated Sorting'; *Materials and manufacturing processes* Volume: 30 Pages: 458-463 (2015)